

Protective Mission against a Highly Maneuverable Rogue Drone Using Defense Margin Strategy

Minjun Sung, Christophe Johannes Hiltebrandt-McIntosh, Hunmin Kim and Naira Hovakimyan

Abstract—The current paper studies a protective mission to defend a domain called the *safe zone* from a rogue drone invasion. We consider a one attacker and one defender drone scenario where only a noisy observation of the attacker at every time step is accessible to the defender. Directly applying strategies used in existing problems such as pursuit-evasion games are shown to be insufficient for our mission. We introduce a new concept of *defense margin* to complement an existing strategy and construct a control strategy that successfully solves our problem. We provide analytical proofs to point out the limitations of the existing strategy and how our defense margin strategy can be used to enhance performance. Simulation results show that our suggested strategy outperforms that of the existing strategy at least by 36.0%*p* in terms of mission success.

I. INTRODUCTION

Along with the rapid growth of the drone market, case reports and consequential concerns about malicious drones have been increasing. Some of the rogue drone incidents include flight interruption [1], terror attacks [2], privacy intrusion [3], and many more. From these incidents, it becomes clear that we need to develop measures to defend property, land, or any protective targets from unauthorized aerial invasions.

Fortunately, there have been numerous researches on tracking and defending moving aerial vehicles. In particular, various detection methods utilizing radio signals, radar, video, audio information, and combinations of these were investigated [4], [5]. Active capturing methods using net guns and birds have been proposed [5]. Jamming methods using Electromagnetic Pulse (EMP) have been explained in [6].

Jamming is an effective neutralization scheme. However, since EMP can cause unintended impacts, most countries prohibit the use of jamming devices at the consumer level [7]. As a result, we need to rely on aerial capturing methods where we need to shoot net bullets from the defender drones to neutralize the malicious drone [7]. To do so, the defender drone must steer close enough to the rogue drone.

In constructing a problem to effectively steer the defender while protecting the *safe zone*, we assume the followings: 1) The objective of the mission accounts for a designated area that we intend to protect. 2) The observation of a rogue

This work has been supported by the National Science Foundation (CNS-1932529) and NASA (NNH20ZEA001N-ULI).

Minjun Sung, Christophe Johannes Hiltebrandt-McIntosh, Hunmin Kim, and Naira Hovakimyan are with the Department of Mechanical Science and Engineering, University of Illinois at Urbana-Champaign, USA. {mjsung2, cjh11, hunmin, nhovakim}@illinois.edu

drone is noisy. 3) The rogue drone is highly maneuverable and its trajectory or dynamics are not known in advance.

To the best of our knowledge, a mission to track and defend a drone most resembles the close-in jamming problem introduced in [8]. This work first addressed the problem to jam a rogue drone with observational uncertainty. However, it has limited the number of possible control actions for agents. More importantly, it differs from our problem in that it does not assume a protective mission and it chiefly focuses on jamming intensity. In our work, we instead assume a protective mission with an aerial capturing scenario where the defender drones have to approach the attacker drone more closely. Other relevant field of research includes differential Pursuit and Evasion (PE) games [9], Perimeter Defense (PD) game [10], and variations of these games. In PE games, a pursuer tries to intercept an evader while an evader tries to avoid a pursuer. This problem has been extensively studied including one pursuer-one evader problem [11]–[13], multi-agent problem [14]–[17], and with observational uncertainty [18]–[21]. This class of problems intends to find conditions for which the pursuer or evader can guarantee its victory, without considering any defense objective. A subclass of PE problem is Target-Attacker-Defender (TAD) game where an evader (attacker) additionally tries to reach the target while evading the pursuer (defender). TAD game assumes limited maneuverability of an attacker or knowledge of an attacker's dynamical model [22], [23]. This is because the TAD game was initially motivated by military missions where such assumptions are reasonable. PD game, on the other hand, limits the defender to only move along the perimeter of the target during its mission, and it is without noise in the observation.

Our main contributions for this work are:

- 1) Novel problem formulation assuming highly maneuverable agents, noisy observation, and the *safe zone*.
- 2) Providing a new metric to quantify defense performance in a protective scenario.
- 3) Designing a defense strategy based on the new metric and proving its efficacy analytically and empirically.

A. Notations used in this work

In this work we denote Euclidean norm as $\|\cdot\|$, expectation of a random variable as $\mathbb{E}[\cdot]$. For geometric analysis in Section III-B, we used $\overline{z_a z_b}$ to denote line segment that connects the two endpoints of the vectors z_a and z_b . Moreover, $z_a \perp z_b$ and $z_a \parallel z_b$ respectively tell that the vectors are perpendicular and parallel to one another.

TABLE I
NOTATIONS

t	Time
Ω_I	Zone of interest
Ω_S	Safe zone
R_{Ω_I}	Radius of Ω_I
R_{Ω_S}	Radius of Ω_S
x_t^a, x_t^d	Attacker (a) and defender (d) state vector $\in \mathbb{R}^2$
e_t	Error vector $x_t^a - x_t^d$
u_t^a, u_t^d	Control input for attacker and defender
w_t	Measurement noise
y_t	Noisy observation of an attacker $x_t^a + w_t$
σ_t	Standard deviation of a measurement noise
τ	Maximum capturing distance
$\rho_{x_t^a}$	Defense margin
λ_t	Weight parameters for defender control
P_t	Observational reliability

II. PROBLEM FORMULATION

The problem in this paper considers a protective mission of a single defending drone, called the defender, against a single attacking drone, called the attacker. The objective of the defender is to prevent an attacker from invading the *safe zone*. This paper focuses to provide an effective defender strategy that can be implemented against a highly maneuverable attacker with unknown trajectory and observational uncertainty. One defender and one attacker scenario can be considered as the smallest module which can be directly extended to multi-agent scenarios as in [24], [25].

A. State-space representation

The mission is assumed to be held in \mathbb{R}^2 space. The zone of interest $\Omega_I \subset \mathbb{R}^2$ is defined to be the region that observation of a drone in this area is considered to have a rogue intent. The safe zone $\Omega_S \subset \Omega_I$ is defined to be a sufficiently large domain that encompasses the target that the defender wishes to defend. The attacker wins the mission if it beats the defender and reach Ω_S . In this work we assume Ω_I, Ω_S to be a circle with respective radius $R_{\Omega_I}, R_{\Omega_S}$ and the origin to be the center of both circles.

An attacker's configuration at time t is denoted as $x_t^a \in \mathbb{R}^2$ and it represents the planar position in Cartesian coordinates. Discrete-time dynamics of the attacker can be written as:

$$x_{t+1}^a = x_t^a + u_t^a. \quad (1)$$

Here $u_t^a \in \mathbb{U}_t^a \subset \mathbb{R}^2$ is a deterministic control input of the attacker, and it is unknown to the defender at all times. Moreover, \mathbb{U}_t^a denotes a set of admissible control of an attacker at time t .

Similarly, a configuration of the defender at time t is expressed as $x_t^d \in \mathbb{R}^2$, and

$$x_{t+1}^d = x_t^d + u_t^d \quad (2)$$

where $u_t^d \in \mathbb{U}_t^d \subset \mathbb{R}^2$ is the defender's deterministic control input, and \mathbb{U}_t^d is the set of possible control actions of the defender at time t .

In practice, u_t^a and u_t^d can be interpreted as a travel distance of an attacker and a defender per unit time, or *speed*. In this paper we assume $\mathbb{U}_t^d = \mathbb{U}_t^a = \{u \in \mathbb{R}^2 : \|u\| \leq 1\}$, such that the attacker and the defender has a same fixed maneuverability. Being able to instantly change directions at any point in time, this condition accounts for the high maneuverability of drones. Moreover, $\|u_t^a\| \leq 1$ and $\|u_t^d\| \leq 1$ is a normalization of a speed with the maximum speed. In our work, the attacker and the defender have an equivalent maximum speed. This is a relaxed assumption used in a handful of papers [18], [26], while many works assume the defender to outpace the attacker [27], [28].

The attacker is considered to be *intercepted* or *captured* by the defender if the distance $\|e_t\| \triangleq \|x_t^a - x_t^d\|$ between the attacker and defender is closer than the maximum capturing distance τ . Formally, the attacker is intercepted if

$$\|e_t\| \leq \tau. \quad (3)$$

There are different sizes and types of net guns, according to which the maximum capturing distance τ can be characterized.

B. Attacker detection model

In PE games with uncertainty, various models including Brownian motion model [19], [21] and ellipsoid model [18] has been considered. In this work, we follow the uncertainty model used in [29] such that we receive independent noisy state observation of the attacker every time step.

An observation of x_t^a at time t is denoted as $y_t \in \mathbb{R}^2$, and is subject to a zero-mean Gaussian noise with covariance matrix $\sigma_t^2 I_2$, where $\sigma_t^2 \in \mathbb{R}_{\geq 0}$ represents a variance of a Gaussian distribution, and the I_2 represents a 2×2 identity matrix [30], [8]. Formally, the following model is adopted to express the observational uncertainty:

$$y_t = x_t^a + w_t \quad (4)$$

$$w_t \sim \mathcal{N}(0, \sigma_t^2 I_2).$$

Lastly, σ_t is modeled by adopting the uncertainty model proposed in [29]:

$$\sigma_t^2 = \beta_b + \beta_d \|e_t\|^2 + \beta_v (1 - \nu_t). \quad (5)$$

Parameters $\{\beta_b, \beta_d, \beta_v\}$ are non-negative real values characterized by the sensor and the estimation model. Specifically, they represent baseline variance, variance coefficient for distance, and variance coefficient for visibility, respectively. Visibility term $\nu_t \in [0, 1]$ relates the blockage of the sight to variance of the uncertainty, such that $\nu_t = 0$ if the sight is fully blocked by an obstacle, and $\nu_t = 1$ if the sight is not blocked at all. Any values between represent partial blockage of the sight.

In this paper, we will consider an environment without any obstacles such that $\nu_t = 1 \forall t$. Furthermore, we will consider zero baseline variance or $\beta_b = 0$ implying that the observational uncertainty becomes zero when the distance from the defender to the attacker is zero. Then, (5) can be rewritten as

$$\sigma_t^2 = \beta \|e_t\|^2 \quad (6)$$

where β is a short hand notation for β_d . As such, we can rewrite (4) with (6) as

$$\begin{aligned} y_t &= x_t^a + w_t \\ w_t &\sim \mathcal{N}(0, \beta \|e_t\|^2 I_2), \end{aligned} \quad (7)$$

completing the description of the attacker detection model.

C. Joint tracking and defending problem

Now we formally state our problem in this section. The defender's mission is to prevent the attacker state from being in the safe zone Ω_S for all time, *or* to intercept the attacker before it reaches the safe zone. Precisely, the problem is to find discrete control input u_t^d such that it satisfies

$$\begin{aligned} x_t^a &\notin \Omega_S \quad \forall t \in [t_i, t_f] \\ \text{Or} \end{aligned} \quad (8)$$

$$\exists t_c \in [t_i, t_f] : (x_t^a \notin \Omega_S \quad \forall t \in [t_i, t_c]) \wedge (\|e_{t_c}\| \leq \tau)$$

subject to

$$\begin{aligned} \|u_t^d\| &\leq 1, \|u_t^a\| \leq 1 \quad \forall t \in [t_i, t_f] \\ y_t &= x_t^a + w_t \\ w_t &\sim \mathcal{N}(0, \beta \|e_t\|^2 I_2) \end{aligned} \quad (9)$$

where t_i , t_f , t_c respectively denote the initial time of observation, terminal time that can be chosen by the user, and the capturing time. Note that this problem is not limited to the interception problem, but defines a more general class of a defense problem. The defender can win also by not letting the attacker to pass through for sufficiently long *runtime*. Fig 1 visualizes the problem.

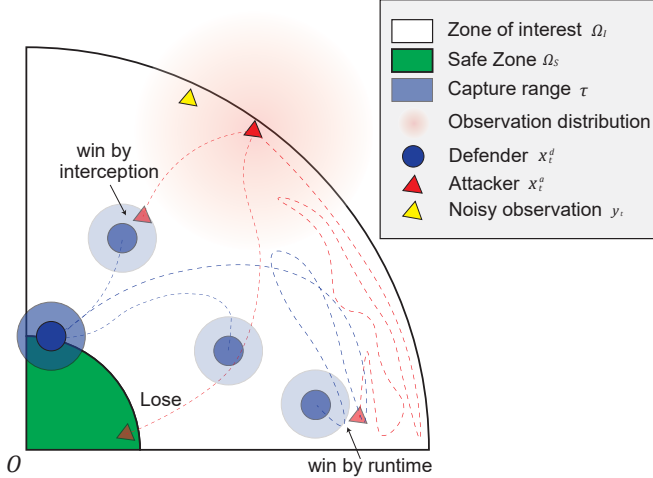


Fig. 1. Problem visualization

III. METHOD

Our solution to the joint tracking and defending problem is partly motivated by the properties of the Pure Pursuit (PP) strategy, which is a widely adopted guidance law for interception missions. We will formally introduce and explain the advantages and limitations of the PP strategy in Section III-A along with other popular guidance laws. As a

result of the subsection, we point out that the PP strategy is insufficient in our mission. In Section III-B we introduce a strategy based on *defense margin* which can complement the PP strategy. Then, in Section III-C we propose a strategy that combines the two strategies to effectively solve our problem.

A. Baseline: Pure Pursuit strategy

Typical and popular strategies utilized in PE games are Constant Bearing (CB), Line of Sight (LoS), and PP guidance laws [31]. CB assumes the knowledge of the attacker's instantaneous velocity as well as its position [32], whereas the defender only has access to noisy observation of the attacker in our problem. Consequently, CB is not suitable to apply for our problem.

LoS, on the other hand, is known to be infeasible in missions with observational uncertainty unless there are external or additional measures to complement the noisy observation [33]. Sufficient support for reliable observation was a reasonable assumption for military missions such as intercepting a missile. However, in this problem, we are assuming a more generic situation where such support is unavailable. This crosses out LoS from our feasible strategy.

Having only access to the instantaneous positional estimate of the attacker, PP strategy is a reasonable strategy to be considered [32]. The idea of this strategy is to always steer the defender directly to the observation of the attacker. This can be considered as a strategy that solely focuses on the second objective of (8). Formally, the defender's control input is designed by

$$u_t^d = \frac{y_t - x_t^d}{\|y_t - x_t^d\|} \quad (10)$$

where u_t^d is normalized to meet the constraint (9) of our problem.

In this work, we show that the PP strategy is an effective strategy, but for limited conditions due to the presence of uncertainty. Here we explain such conditions analytically.

Definition 1. Consider n -dimensional stochastic discrete time system

$$\zeta_{t+1} = f(\zeta_t, \chi_t, \chi), \quad \zeta(t_0) = \zeta_0 \quad (11)$$

The trivial solution of the system is said to be stochastically stable or stable in probability if, for every $\epsilon > 0$ and $h > 0$ there exists $\delta = \delta(\epsilon, h, t_0) > 0$ such that

$$P\{|\zeta_t| < h\} \geq 1 - \epsilon, \quad t \geq t_0 \quad (12)$$

when $|\zeta_0| < \delta$. Otherwise, it is said to be stochastically unstable [34].

Consider Lyapunov function $V : \mathbb{R}^n \rightarrow \mathbb{R}$, with $V(0) = 0$. Its discrete increment is expressed as follows:

$$\Delta V(\zeta_t) = V(\zeta_{t+1}) - V(\zeta_t) \quad (13)$$

Using this definition and notation of discrete Lyapunov function and its increment, following theorems are derived:

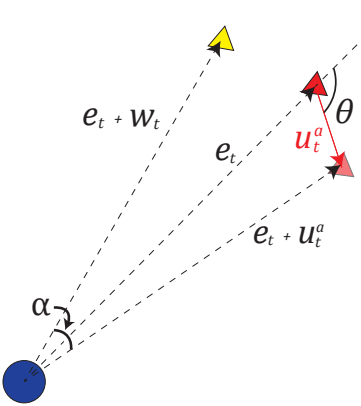


Fig. 2. Visualization of notations and notions used in Theorem III.2

Theorem III.1. *If there exists a positive definite function $V(\zeta_t) \in C^2(D_r)$, such that*

$$E[\Delta V(\zeta_t)] \leq 0 \quad (14)$$

for all $\zeta_t \in D_r$, then the trivial solution of (11) is stochastically stable in probability [34].

If we consider ζ_t in (14) to be e_t , we can interpret stochastic stability as the defender state converging to that of the attacker. In other words, stochastic stability of e_t implies that the defender is expected to intercept the attacker. In the following, we provide the condition that guarantees such convergence when using the PP strategy.

Theorem III.2. *Assume $\|e_t\| > \sqrt{2}$ and $\|w_t\| < \|e_t\|$. The error e_t is stable in probability under the PP strategy (10) if the following condition holds:*

$$\frac{e_t^\top u_t^a + 1}{\|e_t + u_t^a\|} \leq \mathbb{E}[\cos \alpha] \quad (15)$$

where

$$\cos \alpha \triangleq \frac{(e_t + w_t)^\top (e_t + u_t^a)}{\|e_t + w_t\| \|e_t + u_t^a\|}, \quad \alpha \in (-\frac{\pi}{2}, \frac{\pi}{2}).$$

Proof. We use the Lyapunov function to provide a condition under which stability can be guaranteed.

Define a Lyapunov function $V(e_t)$ as a dot product of e_t to itself:

$$V(e_t) = e_t^\top e_t. \quad (16)$$

By construction, $V(e_t)$ is positive definite, and $V(0) = 0$. Plugging uncertain observation model (7) to PP control (10) yields:

$$u_t^d = \frac{y_t - x_t^d}{\|y_t - x_t^d\|} = \frac{e_t + w_t}{\|e_t + w_t\|} \quad (17)$$

Plugging (17) into (13), we have

$$\begin{aligned} \Delta V(e_t) &= V(e_{t+1}) - V(e_t) \\ &= (e_t - \frac{e_t + w_t}{\|e_t + w_t\|} + u_t^a)^\top (e_t - \frac{e_t + w_t}{\|e_t + w_t\|} + u_t^a) \\ &\quad - e_t^\top e_t \\ &= -2 \frac{e_t^\top (e_t + w_t)}{\|e_t + w_t\|} + 2 e_t^\top u_t^a + \frac{(e_t + w_t)^\top (e_t + w_t)}{\|e_t + w_t\|^2} \\ &\quad + u_t^{a\top} u_t^a - 2 \frac{(e_t + w_t)^\top u_t^a}{\|e_t + w_t\|} \end{aligned} \quad (18)$$

Rearranging and taking expectation on both side yields,

$$\begin{aligned} \mathbb{E}[\Delta V(e_t)] &= \\ &\quad - 2\mathbb{E}\left[\frac{(e_t + w_t)^\top (e_t + u_t^a)}{\|e_t + w_t\|}\right] + \mathbb{E}\left[\frac{(e_t + w_t)^\top (e_t + w_t)}{\|e_t + w_t\|^2}\right] \\ &\quad + 2\mathbb{E}[e_t^\top u_t^a] + \mathbb{E}[u_t^{a\top} u_t^a] \\ &\leq -2\mathbb{E}\left[\frac{\|e_t + w_t\| \|e_t + u_t^a\| \cos \alpha}{\|e_t + w_t\|}\right] \\ &\quad + 2 e_t^\top u_t^a + 2 \\ &= -2\|e_t + u_t^a\| \mathbb{E}[\cos \alpha] + 2 e_t^\top u_t^a + 2 \end{aligned} \quad (19)$$

Here we simply used $\|u_t^a\| \leq 1$. In addition, $\alpha \in (-\frac{\pi}{2}, \frac{\pi}{2})$ due to $\|e_t\| > \sqrt{2}$ and $\|w_t\| < \|e_t\|$.

Rearranging (19) to satisfy (14), we obtain (15), completing the proof. \square

Remark 1. *Stochastic stability of trivial case (u_t^a being a zero vector) can be directly proved after (18) simply by plugging in u_t^a a zero vector and using $\|e_t\| > \sqrt{2}$ and $\|w_t\| < \|e_t\|$.*

For the PP strategy to be effective, we need the left hand side of (15) to be small and the right hand side to be large. To illustrate this point, implicitly define θ by

$$\cos \theta \triangleq \frac{e_t^\top u_t^a}{\|e_t\| \cdot \|u_t^a\|}, \quad \theta \in [-\pi, \pi].$$

Consider a case $\cos \theta = -1$ and $\|u_t^a\| = 1$ such that $e_t^\top u_t^a = -\|e_t\|$, for which the attacker is moving directly towards the defender. Then, the left hand side of (15) becomes $\frac{-\|e_t\| + 1}{\|e_t\| - 1} = -1$. This makes the inequality to be always true regardless of α . On the other hand, large $\cos \alpha$ can be obtained when we have sufficiently small $\|e_t\|$ in addition to $\cos \theta \simeq -1$. That is because small $\|e_t\|$ will yield $e_t + w_t \rightarrow e_t$ by (9), and $\cos \theta \simeq -1$ will yield $\kappa e_t \simeq e_t + u_t^a$ where $\kappa \in (0, 1]$ is a constant. This consequently makes $\cos \alpha \rightarrow 1$ to make the inequality to always hold.

The PP strategy becomes sufficiently more effective when $\cos \theta \simeq -1$. However, since the defender do not know the precise position of the attacker, small $\|e_t\|$ to induce $w_t \simeq 0$ need to be leveraged simultaneously. In other words, the defender would have to behave in a *conservative* manner until small $\|e_t\|$ is achieved, and then utilize PP strategy.

Remark 2. Note that if $\theta = 0$, the attacker is heading directly away from the defender. For $\|u_t^a\| = 1$ the left hand side of (15) becomes 1. The inequality does not hold almost surely. This agrees with our intuition that if the attacker is moving away from the defender, the best pursuit a defender can do is to keep $\|e_t\|$ constant, as long as the maximum speed of a defender and an attacker are equivalent.

B. Complement: Defense Margin Strategy

The limitation of PP guidance law makes it insufficient to be applied to our mission. In particular, the goal of the PP strategy corresponds only to the second objective in (8). Now that our problem additionally considers a safe zone (the first objective in (8)), we try to design a strategy that accounts for this objective. As such, in this subsection, we explain a safe reachable set and apply this to suggest a new metric *defense margin* which measures a defense performance at each state. Then, we introduce a Defense Margin strategy (DM strategy) and explain how this can complement PP strategy.

Definition 2. Safe reachable set $L_{x_t^a}$ is the set of positions reachable by the attacker before the defender [18].

Following the assumption in (9) that the defender is at least as fast as the attacker, we can express $L_{x_t^a}$ as follows:

$$L_{x_t^a} = \{l \in \mathbb{R}^2 \mid \|l - x_t^a\| \leq \|l - x_t^d\|\}. \quad (20)$$

Geometrically, the safe reachable set is the half-plane, points in which are closer to the attacker than the defender.

Having (20), we can subsequently define $l_{x_t^a} \in L_{x_t^a}$ the closest point in reachable set to the safe zone:

$$l_{x_t^a} = \arg \inf_{l \in L_{x_t^a}} \|\Omega_S - l\| \quad (21)$$

where $\|\Omega_S - l\| \triangleq \inf_{\omega_S \in \Omega_S} \|\omega_S - l\|$, for a given l .

Finally, we can define new metric *defense margin* as follows:

Definition 3. Defense margin $\rho_{x_t^a}$ is defined as the norm of $l_{x_t^a}$:

$$\rho_{x_t^a} = \|l_{x_t^a}\|. \quad (22)$$

Note that if $\rho_{x_t^a} \leq R_{\Omega_S}$, there exists a strategy for the attacker to reach the safe zone regardless of the defender strategy.

Using the concept of defense margin, we propose the following strategy, or namely *Defense margin (DM) strategy*:

$$u_t^d = \frac{l_y - x_t^d}{\|l_y - x_t^d\|} \quad (23)$$

where l_y is defined by replacing x_t^a with y_t in (21).

Intuitively, the DM strategy makes the defender maneuver to the closest point from the safe zone that an attacker can possibly reach. This can be considered as a strategy to implicitly accomplish the first goal of (8) by enforcing the attacker to take a longer detour to reach the safe zone.

Lemma III.3. Defense margin $\rho_{x_t^a}$ can be measured with following equation

$$\rho_{x_t^a} = \frac{1}{2} \frac{\|x_t^a\|^2 - \|x_t^d\|^2}{\|x_t^a - x_t^d\|}. \quad (24)$$

Proof. Recall that $l_{x_t^a}$ is a vector in the half-plane $L_{x_t^a}$ that has a minimum distance to the origin. Moreover, $(\frac{x_t^d + x_t^a}{2} - l_{x_t^a}) \perp (x_t^a - x_t^d)$ or equivalently,

$$\left(\frac{x_t^d + x_t^a}{2} - l_{x_t^a}\right) \cdot (x_t^a - x_t^d) = 0 \quad (25)$$

which yields

$$\left(\frac{x_t^d + x_t^a}{2}\right) \cdot (x_t^a - x_t^d) = l_{x_t^a} \cdot (x_t^a - x_t^d). \quad (26)$$

Equivalently,

$$\frac{\|x_t^a\|^2 - \|x_t^d\|^2}{2} = \|l_{x_t^a}\| \|x_t^a - x_t^d\| \quad (27)$$

where the right hand side holds since $l_{x_t^a} \parallel x_t^a - x_t^d$. Solving for $\|l_{x_t^a}\|$ yields,

$$\rho_{x_t^a} = \|l_{x_t^a}\| = \frac{1}{2} \frac{\|x_t^a\|^2 - \|x_t^d\|^2}{\|x_t^a - x_t^d\|}. \quad (28)$$

□

In the following, we provide an analytical proof to explain that (23) outperforms (10) in terms of defense margin, implying that (23) can complement (10).

Theorem III.4. Assume $\|e(t)\| > \sqrt{2}$ and $\|x_t^a\| > \|x_t^d\|$. For static attacker state vector $x_{t+1}^a = x_t^a$ with uncertainty $w_t = 0 \forall t$, following inequality holds for one step change of the defense margin:

$$\Delta \rho_{x_t^a} | u_{DM}^d \geq \Delta \rho_{x_t^a} | u_{PP}^d \quad (29)$$

where $\Delta \rho_{x_t^a} | u_{DM}^d$ and $\Delta \rho_{x_t^a} | u_{PP}^d$ denotes for $\Delta \rho_{x_t^a}$ following DM strategy (23) and PP strategy (10), respectively.

Proof. The proof is explained in three blocks:

- 1) Execute a coordinate transformation for computational simplicity
- 2) Show that the change in defense margin for PP strategy is precisely $\frac{1}{2}$, or formally $\Delta \rho_{x_t^a} | u_{PP}^d \equiv \frac{1}{2}$
- 3) Show that $\Delta \rho_{x_t^a} | u_{PP}^d \geq \frac{1}{2}$

1) Coordinate Transformation At time t given x_t^a and x_t^d , we do a *rigid* coordinate transformation $\Phi : x \rightarrow \hat{x}$ such that $x_t^d \rightarrow \hat{x}_t^d = [0, 0]^\top$, $x_t^a \rightarrow \hat{x}_t^a = [r, 0]^\top$ where $r = \|e(t)\|$ and the center of the safe zone Ω_S will correspondingly be transformed to $[p, q]^\top$. The assumption $\|x_t^a\| > \|x_t^d\|$ is translated to

$$p < \frac{r}{2} \quad (30)$$

in the transformed coordinate.

Rigid transformation only allows rotation and followed by translation, and therefore preserves the Euclidean distance between every pair of points. In this transformed coordinate, the two strategies are simplified as $u_{PP}^d = [1, 0]^\top$, and

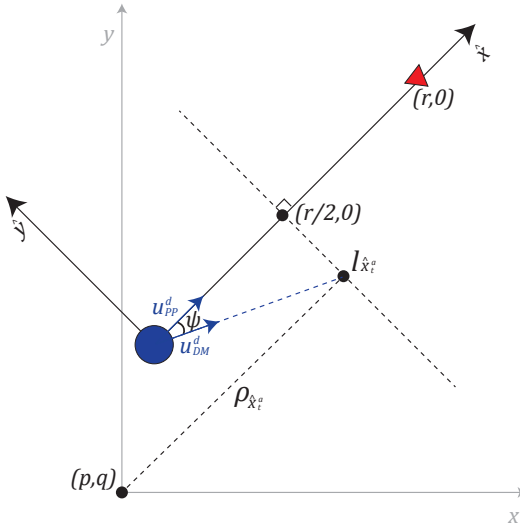


Fig. 3. Visualization of notations and notions used in Theorem III.4

$u_{DM}^d = [\cos \psi, \sin \psi]^\top$. In other words, $x_{t+1}^d = [1, 0]^\top$ for PP strategy, and $x_{t+1}^d = [\cos \psi, \sin \psi]^\top$ for DM strategy.

Now $\rho_{\hat{x}_t^a}$ lies precisely on the perpendicular bisector of the line segment $\hat{x}_t^a \hat{x}_t^d$. Consequently, $\angle \rho_{\hat{x}_t^a} \hat{x}_t^d \hat{x}_t^a = \angle \rho_{\hat{x}_t^a} \hat{x}_t^a \hat{x}_t^d = \psi$ where $\psi \in (-\frac{\pi}{2}, \frac{\pi}{2})$. Formally, following holds:

$$p = \frac{r}{2} - \rho_{\hat{x}_t^a} < \frac{r}{2} \quad (31)$$

$$q = \frac{r}{2} \tan \psi. \quad (32)$$

2) Change in Defense Margin for PP strategy

From (31) we have $\rho_{\hat{x}_t^a} = \frac{r}{2} - p$. For $x_{t+1}^d = [1, 0]^\top$, we obtain $\rho_{\hat{x}_{t+1}^a} = \frac{r+1}{2} - p$. Consequently,

$$\begin{aligned} \Delta \rho_{\hat{x}_t^a} |u_{PP}^d| &= \rho_{\hat{x}_{t+1}^a} - \rho_{\hat{x}_t^a} \\ &= \left(\frac{r+1}{2} - p\right) - \left(\frac{r}{2} - p\right) = \frac{1}{2}. \end{aligned} \quad (33)$$

3) Change in Defense Margin - Our strategy

Similar to (33), to obtain $\rho_{\hat{x}_{t+1}^a}$ we will need to find a distance from $[p, q]^\top$ to the straight line that bisects $\hat{x}_{t+1}^d = [\cos \psi, \sin \psi]^\top$ and $[r, 0]^\top$ or equivalently,

$$\frac{r - \cos \psi}{\sin \psi} \left(x - \frac{r + \cos \psi}{2}\right) - \left(y - \frac{\sin \psi}{2}\right) = 0. \quad (34)$$

The distance from $[p, q]^\top$ to (34) can be obtained with the following equation:

$$\rho_{\hat{x}_{t+1}^a} |u_{DM}^d| = \frac{|r^2 - 1 + 2q \sin \psi - 2p(r - \cos \psi)|}{2\sqrt{(r - \cos \psi)^2 + \sin^2 \psi}}. \quad (35)$$

Here we will find the lower bound of $\rho_{\hat{x}_{t+1}^a} |u_{DM}^d|$ and assert that it is greater or equal to $\frac{1}{2}$ to complete our proof.

First observe that we only need to consider for $\psi \in [0, \frac{\pi}{2}]$ since $\rho_{\hat{x}_{t+1}^a}$ is symmetrical with respect to the \hat{x} -axis. Every result we obtain can therefore be identically proved for $\psi \in (-\frac{\pi}{2}, 0]$. Subsequently, $q \geq 0$ by (32). Note that $q = 0$

or $\psi = 0$ is a trivial case which yields $u_{PP}^d \equiv u_{DM}^d$. This obviously makes $\Delta \rho_{\hat{x}_t^a} |u_{PP}^d| \equiv \Delta \rho_{\hat{x}_t^a} |u_{DM}^d| = \frac{1}{2}$.

The numerator of (35) can be lower-bounded by the following:

$$\begin{aligned} r^2 - 1 + 2q \sin \psi - 2p(r - \cos \psi) &> r^2 - 1 + 2q \sin \psi - 2p(r - \cos \psi) |p| = \frac{r}{2} \\ &= -1 + 2q \sin \psi + r \cos \psi \\ &= -1 + \frac{r}{\cos \psi} > 0 \quad \forall \psi \in [0, \frac{\pi}{2}). \end{aligned} \quad (36)$$

Here we used $\psi \in [0, \frac{\pi}{2})$, $r > \sqrt{2}$, $q = \tan \psi$, and $p < \frac{r}{2}$. Hence, we can ignore the absolute operator for the remainder of the proof.

Rewriting (35) yields

$$\begin{aligned} \rho_{\hat{x}_{t+1}^a} |u_{DM}^d| &= \frac{|r^2 - 1 + 2q \sin \psi - 2p(r - \cos \psi)|}{2\sqrt{(r - \cos \psi)^2 + \sin^2 \psi}} \\ &> \frac{r^2 - 1 + 2q \sin \psi - r(r - \cos \psi)}{2\sqrt{(r - \cos \psi)^2 + \sin^2 \psi}} \\ &= \frac{r - \cos \psi}{2 \cos \psi \sqrt{(r - \cos \psi)^2 + \sin^2 \psi}}. \end{aligned} \quad (37)$$

Here last equality again used $p < \frac{r}{2}$ and $q = \frac{r}{2} \tan \psi$.

Furthermore,

$$\frac{r - \cos \psi}{2 \cos \psi \sqrt{(r - \cos \psi)^2 + \sin^2 \psi}} \geq \frac{1}{2} \quad (38)$$

holds whenever $r > \sqrt{2}$. Note that equality holds only when $\psi = 0$. Finally, Due to the rigidity of the transformation $\Phi(x, y)$, we can obtain $\rho_{\hat{x}_{t+1}^a} |u_{DM}^d| \geq \rho_{\hat{x}_{t+1}^a} |u_{PP}^d|$ directly from $\rho_{\hat{x}_{t+1}^a} |u_{DM}^d| \geq \rho_{\hat{x}_{t+1}^a} |u_{PP}^d|$, completing the proof. \square

Remark 3. Unlike the PP strategy, goal of which is to capture the attacker, the DM strategy has different goal to maximize the defense margin. Therefore, it is inadequate to conduct stability analysis for the DM strategy as in Theorem III.2. \blacksquare

This theorem asserts that the DM strategy takes the safe zone into account and therefore it can be used to complement the PP strategy. Empirical extension of Theorem III.4 is discussed in Section IV.

Although DM strategy is expected to be better than PP strategy in terms of defense margin, the defense margin is not guaranteed to be non-decreasing. Together with the fact that DM strategy does not explicitly steer to intercept the defender, solely relying on DM strategy can lead to a shrinking defense margin without an interception. In other words, since DM strategy only accounts for the first objective of (8), it shall be used together with the PP strategy to best solve for our problem.

C. Combination: Adjusted Defense Margin Strategy

We have discussed the limitations of using PP and DM strategy in Section III-A and III-B respectively. Since we only need to accomplish either one of the two goals in (8), relying exclusively on PP or DM is not sufficient. In this subsection, we introduce a parameterized combination of the two to increase the defense performance.

To this end, we introduce a weight parameter λ_t and define *Adjusted Defense Margin (ADM) strategy* as follows:

$$u_t^d = c\lambda_t \frac{y - x_t^d}{\|y - x_t^d\|} + c(1 - \lambda_t) \frac{l_\mu - x_t^d}{\|l_\mu - x_t^d\|} \quad (39)$$

where c is a constant to make $\|u_t^d\| = 1$. Note here that $\lambda_t \equiv 1$ and $\lambda_t \equiv 0$ represents the PP and DM strategy.

We want to design λ_t such that it captures the evolving nature of a mission. For instance, when $\cos \theta \simeq -1$ and $\|e_t\|$ is small enough, PP strategy becomes a more effective strategy as it is discussed in Section III-A. As such, we intend to design a strategy that first chiefly follows a DM strategy which can steer the defender to a more favorable position to apply PP strategy. Then, as $\|e_t\|$ gets smaller, we can tend more to the PP strategy to intercept the attacker. Now the problem is to construct λ_t that does this job.

We first define the reliability of an observation y_t which we can utilize without precise x_t^a .

Definition 4. Let \hat{w}_t be an estimate of uncertainty w_t and is expressed as

$$\hat{w}_t \sim \mathcal{N}(0, \beta(\|y_t - x_t^d\|^2 I_2)). \quad (40)$$

Reliability of observation y_t is denoted as P_t and expressed as follows:

$$P_t = F(k, k) + F(-k, -k) - F(-k, k) - F(k, -k). \quad (41)$$

Here $F(\cdot, \cdot) : \mathbb{R} \times \mathbb{R} \rightarrow \mathbb{R}$ is cumulative distribution function (CDF) of a multivariate Gaussian distribution \hat{w}_t and k is the characterizing length of the reliability square.

In the above definition, we are creating a square of length $2k$, the center of which is the observation y_t . Then we obtain a probability of the target being inside the square by integrating multivariate Gaussian distribution within the square while the variance of the distribution is $\beta\|y_t - x_t^d\|^2 I_2$. Here we are trying to make the control decision based on y_t as if it is x_t^a , which is known as *certainty equivalence approach* [35].

Remark 4. One might argue that it would be more mathematically rigorous to use integration over multivariate Gaussian distribution within a fixed radius instead of a square. However, (41) is known to be a good approximation [36], [37] and the computation can be done in time complexity of $O(1)$, which is a substantial advantage in real-time missions.

Utilizing the reliability of an observation, we propose the following parameterization:

$$\lambda_t = P_t. \quad (42)$$

Rewriting (39) with (42), we obtain

$$u_t^d = cP_t \frac{y - x_t^d}{\|y - x_t^d\|} + c(1 - P_t) \frac{l_\mu - x_t^d}{\|l_\mu - x_t^d\|}. \quad (43)$$

Consider a case without observational noise, i.e. $\beta = 0$. This automatically makes $P_t \equiv 1$, reducing (43) to (10). In other words, if we have accurate information about the attacker at all times, we follow the PP strategy. When the uncertainty is large, we tend more to the DM strategy.

IV. SIMULATION AND RESULTS

In this section, we present a performance comparison of the strategies discussed in this paper. To this end, we first describe the parameters and different types of attacker behaviors used in the simulation. Then we provide and explain simulation results. To obtain further insight, we introduce a function approximator of $\Delta\rho_{x_t^a}$ using Neural Network (NN) to extend the result of Theorem III.4.

Simulation of the defenders using PP strategy (10), DM strategy (23), and ADM strategy (43) were tested against three different behaviors of attackers: **1) Linear**, **2) Spiral**, and **3) Intelligent**. Linear strategy is a strategy that simply steers to the origin, or $u_{\text{Linear}}^a = -\frac{x^a}{\|x^a\|}$. Specific details and algorithms for the other two behaviors are explained in the Algorithm 1.

Algorithm 1 Attacker behaviors

Spiral behavior

```

 $x, y \leftarrow x^a$ 
 $r \leftarrow \|x^a\|$ 
 $\phi \leftarrow \arctan y/x$ 
 $d\phi \leftarrow 1/r$ 
 $\phi \leftarrow \phi - d\phi$ 
 $x_2 \leftarrow (r - 1) \cos d\phi - x$ 
 $y_2 \leftarrow (r - 1) \sin d\phi - y$ 
 $u^a \leftarrow [x_2 - x, y_2 - y]/\|[x_2 - x, y_2 - y]\|$ 
 $x^a \leftarrow x^a + u^a$ 

```

Intelligent behavior

$w \sim \mathcal{N}(0, \beta\ e_t\ ^2 I_2)$	
$\hat{x}^d \leftarrow x^d + w$	▷ Noisy observation
$d_1 \leftarrow -(\hat{x}^d - x^a)/\ \hat{x}^d - x^a\ $	▷ Evade defender
$d_2 \leftarrow -x^a/\ x^a\ $	▷ Steer to the origin
$k_1 \leftarrow 1/\ \hat{x}^d - x^a\ $	
$k_2 \leftarrow 1$	
$x^a = x^a + (k_1 d_1 + k_2 d_2)/\ k_1 d_1 + k_2 d_2\ $	

Linear and spiral behavior are predefined controls that follow a straight line or spiral curve (clock-wise) to the safe zone, and an intelligent behavior steers an attacker based on its noisy observation of the defender. Unlike the other two, intelligent strategy behaves *in reaction to* the defender. Figure 4 will give visual intuition of how attacker behaviors are designed.

Table II summarizes the parameters used in the simulation.

TABLE II
PARAMETERS USED IN SIMULATION

Notation	Description	Value
t_f	Terminal time	∞
R_{Ω_I}	Radius of the region of interest	50
R_{Ω_S}	Radius of the safe zone	10
τ	Maximum range of interception	2
Λ^d	Distribution of a defender's initial position $x_{t_i}^d$ in polar coordinate system	$(\mathcal{U}[0, 20], \mathcal{U}[-\pi, \pi])$
Λ^a	Distribution of an attacker's initial position $x_{t_i}^a$ in polar coordinate system	$(\mathcal{U}[45, 50], \mathcal{U}[-\pi, \pi])$
β	Coefficient for variance of uncertainty	0.05
k	Characterizing length of a square in (41)	0.5

In Table II, Λ^a and Λ^d were introduced to randomly initialize the agents, and \mathcal{U} denotes a uniform distribution. All the values are normalized, therefore they are dimensionless.

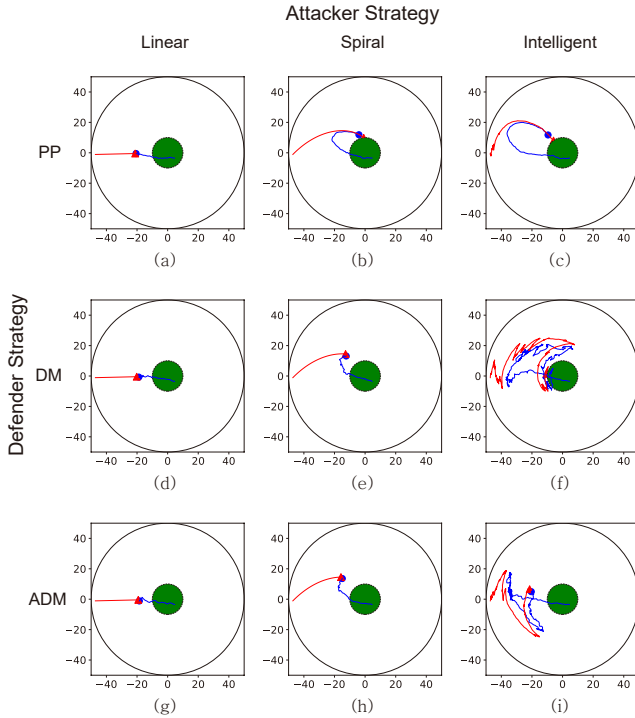


Fig. 4. Trajectories of an attacker and a defender under various behavior scenarios. Outer circle represents region of interest Ω_I and green circle represents safe zone Ω_S . Red and blue lines respectively denote the attacker x_t^a and the defender x_t^d trajectories over time. All cases in this figure have homogeneous initial positions of an attacker and a defender $(x_{t_i}^d, x_{t_i}^a)$. A defender has successfully defended the safe zone in all cases but (b), (c) and (f).

Figure 4 illustrates a trajectory history of nine different case scenarios obtained by three defender strategies and three attacker strategies. The result in the figure specifically is showing a case that the PP guidance law fails to defend the safe zone against spiral (b) and intelligent (c) attacker behavior. The DM strategy exhibited failure at the mission against an intelligent attacker (f), and finally, our proposed ADM

strategy has successfully defended all types of attackers.

We can interpret the same nine cases in terms of $\rho_{x_t^a}$. In Figure 5, we can point out the attacker-winning cases of Figure 4 (b), (c), (f), for which $\rho_{x_t^a}$ eventually reaches $R_{\Omega_S} = 10$. Noticeably for Figure 5 (b) and (c), $\Delta\rho_{x_t^a}|u_{DM}^d \geq \Delta\rho_{x_t^a}|u_{PP}^d$ as in (29). Take (b) for example. Both defense strategies maintained a roughly same defense margin until 10-th timestep. However, once the attacker beats around the defender that follows the PP strategy, defense margin plummets until the attacker finally wins the game. In the meanwhile for the defender following the DM strategy, the defense margin is maintained above the initial value until it intercepts the attacker at around 35-th timestep.

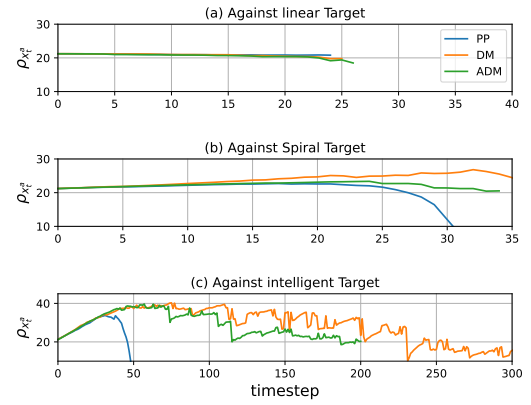


Fig. 5. Defense margin as a function of timestep. The mission is considered to have failed if $\rho_{x_t^a} = R_{\Omega_S} = 10$. Trajectories that ended before failing implies that the defender has intercepted the attacker.

Yet, Figure 5 (a) and (c) needs further explanation. In (a) all the strategies maintained about the same defense margin and all captured the attacker at around the 25-th time step. To be specific, all three strategies behaved similar to the others because $\psi \simeq 0$. This is clear in Figure 4 (a), (d), (g). Even though we can in general expect from (29) that the DM strategy outperforms PP strategy regarding defense margin, this may not be true in some time steps depending on the attacker behavior and uncertainty.

In addition, Figure 5 (c) portrays a situation where the DM strategy failed its mission although it seemed to obtain largest $\rho_{x_t^a}$ among all strategies. This can be explained by the passivity of the DM strategy. As discussed in Section III-B, DM strategy only accounts for the first objective of (8) without considering the other. As a result, it has only extended the time duration of the mission, without capturing the attacker even when it had chances to do so. An intelligently steering attacker could beat the defender taking advantage of its passivity. On the contrary, ADM strategy intercepted the attacker around the 200-th time step which could successfully complete the mission.

Figure 6 shows a defense performance obtained by running 1,000 trials for each scenarios. 1,000 different randomized initial conditions were saved and applied for all scenarios for fair comparison.

In this figure, we can see some interesting features of

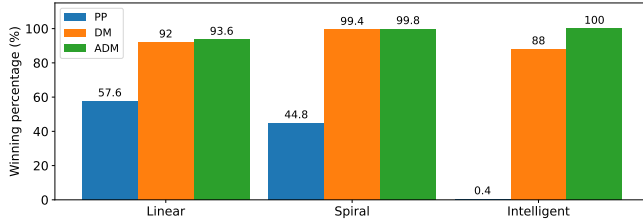


Fig. 6. Winning percentage of each strategies against different attacker strategies. Each percentage results are obtained by counting successful missions out of 1,000 randomly initialized scenarios.

each defense strategy. PP strategy exhibits a decrease in performance with larger complexity of the attacker strategy, whereas DM strategy peaked its performance against the Spiral attacker behavior. Lastly, the ADM strategy performed better with higher complexity of attacker behavior.

Explaining for performance drop of PP strategy is straightforward. As mentioned in Section III-A, this strategy can succeed when Theorem III.2 holds. For instance, Figure 4 (b) and (c) illustrates a case that once $e_t^\top u_t^a \simeq 1$ as in Remark 2, PP strategy becomes helpless. In particular, intelligent attacker could cleverly steer to reach such condition 996 times out of 1000 trials.

DM strategy is designed to complement such limitations of PP strategy. As a result, DM achieves much higher performance than the PP strategy in all scenarios. However, we can see its limitation in Figure 4 (f) in which its passivity culminated in mission failure. As such, the performance of DM strategy necessarily drops against an intelligent attacker.

ADM strategy combines the two strategies and successfully increased the performance. Some of the failure cases can be explained by the randomness of the initial conditions. A number of bipolar initial conditions of an attacker and a defender guaranteed the attacker to win the mission regardless of a defender strategy. In other words, the attacker was closer to the safe zone than the defender. For these cases, linear attacker behavior is the optimal solution for an attacker, and therefore, the ADM strategy had a lower performance against a lower attacker behavior complexity.

Next, we aim to extend Theorem III.4 via numerical simulation. Theorem III.4 assumed absence of uncertainty w_t for simplicity. Here we use a Neural Network to approximate for $\Delta\rho_{x_t^a}$ and analyze results without such assumption.

Definition 5. Assume $u_t^a = -\frac{x_t^a}{\|x_t^a\|}$. A strategy u_A^d is said to be safer than strategy u_B^d with respect to uncertainty if

$$\Delta(\rho_{x_t^a})|_{u_A^d} \geq \Delta(\rho_{x_t^a})|_{u_B^d} \quad (44)$$

where u_A^d and u_B^d relies on uncertain observation of x_t^a .

To compare $\Delta\rho_{x_t^a}|_{u_{PP}^a}$ and $\Delta\rho_{x_t^a}|_{u_{DM}^a}$ in the presence of uncertainty, we trained two fully-connected neural network (FCNN) $\Delta\rho_{\hat{x}_t^a}|_{u_{PP}^a}$ and $\Delta\rho_{\hat{x}_t^a}|_{u_{DM}^a}$ both of which takes (x_t^a, x_t^d) as an argument and respectively return a prediction of $\Delta\rho_{x_t^a}|_{u_{PP}^a}$ and $\Delta\rho_{x_t^a}|_{u_{DM}^a}$. The training data $\{(x_i^a, x_i^d), \Delta\rho_{x_i^a}\}_i^N$ is collected while simulating to obtain

Figure 6 against linear attacker behavior. Here N is the total number of data collected. FCNN has 2 hidden layers of 100 nodes, learning rate of 0.001, and we used Adam optimizer for our work. To test the model, we randomly generated test data samples $(x_i^a, x_i^d)_i^M$, where M is the number of test data samples. Here x_i^a and x_i^d are uniformly sampled from a circle of random radius $\|x_t^a\| \sim \mathcal{U}[25, 40]$ and $\|x_t^d\| \sim \mathcal{U}[0, 15]$, respectively. In this work we used $M = 100,000$.

The following table shows the result of the test:

	PP	DM
$\Delta\rho_{\hat{x}_t^a}$	-0.132	-0.028

This again shows that $\Delta\rho_{x_t^a}|_{u_{DM}^a} \geq \Delta\rho_{x_t^a}|_{u_{PP}^a}$ even in the presence of uncertainty w_t .

V. CONCLUSION

This work introduces a new metric called defense margin to solve for a protective UAV mission in which observation of the attacker is noisy. We provided an analytical proof to justify the implementation of the control strategy based on the defense margin. Finally, empirical results validates the efficacy of the strategy.

Future research avenues shall include methods to tune for optimal parameters according to sensitivity of each parameters to the defense performance. Extension to a multi-agent problem, adding obstacles in the environment, implementation in a 3D environment can also be part of future works. Lastly, various attacker behaviors could be designed and implemented for more comprehensive and reliable simulation results.

REFERENCES

- [1] M. R. Brust, G. Danoy, P. Bouvry, D. Gashi, H. Pathak, and M. P. Gonçalves, “Defending against intrusion of malicious UAVs with networked UAV defense swarms,” in *2017 IEEE 42nd conference on local computer networks workshops (LCN workshops)*. IEEE, 2017, pp. 103–111.
- [2] J. Loeb, “Exclusive: Anti-drone technology to be tested in UK amid terror fears,” *Engineering & Technology*, vol. 12, no. 3, pp. 9–9, 2017.
- [3] A. Singh, D. Patil, and S. Omkar, “Eye in the sky: Real-time drone surveillance system (DSS) for violent individuals identification using scatternet hybrid deep learning network,” in *Proceedings of the IEEE Conference on Computer Vision and Pattern Recognition Workshops*, 2018, pp. 1629–1637.
- [4] B. Taha and A. Shoufan, “Machine learning-based drone detection and classification: State-of-the-art in research,” *IEEE access*, vol. 7, pp. 138 669–138 682, 2019.
- [5] I. Guvenc, F. Koohifar, S. Singh, M. L. Sichitiu, and D. Matolak, “Detection, tracking, and interdiction for amateur drones,” *IEEE Communications Magazine*, vol. 56, no. 4, pp. 75–81, 2018.
- [6] X. Shi, C. Yang, W. Xie, C. Liang, Z. Shi, and J. Chen, “Anti-drone system with multiple surveillance technologies: Architecture, implementation, and challenges,” *IEEE Communications Magazine*, vol. 56, no. 4, pp. 68–74, 2018.
- [7] S. Park, H. T. Kim, S. Lee, H. Joo, and H. Kim, “Survey on anti-drone systems: Components, designs, and challenges,” *IEEE Access*, vol. 9, pp. 42 635–42 659, 2021.
- [8] P. Valiati, S. Papaioannou, P. Kolios, and G. Ellinas, “Multi-agent coordinated close-in jamming for disabling a rogue drone,” *IEEE Transactions on Mobile Computing*, 2021.
- [9] R. Isaacs, *Differential games: a mathematical theory with applications to warfare and pursuit, control and optimization*. Courier Corporation, 1999.
- [10] D. Shishika and V. Kumar, “A review of multi agent perimeter defense games,” in *International Conference on Decision and Game Theory for Security*. Springer, 2020, pp. 472–485.

- [11] Y. Ho, A. Bryson, and S. Baron, "Differential games and optimal pursuit-evasion strategies," *IEEE Transactions on Automatic Control*, vol. 10, no. 4, pp. 385–389, 1965.
- [12] L. Meier, "A new technique for solving pursuit-evasion differential games," *IEEE Transactions on Automatic Control*, vol. 14, no. 4, pp. 352–359, 1969.
- [13] G. Leitmann, "A simple differential game," *Journal of Optimization Theory and Applications*, vol. 2, no. 4, pp. 220–225, 1968.
- [14] P. Hagedorn and J. Breakwell, "A differential game with two pursuers and one evader," *Journal of Optimization Theory and Applications*, vol. 18, no. 1, pp. 15–29, 1976.
- [15] Z. E. Fuchs, P. P. Khargonekar, and J. Evers, "Cooperative defense within a single-pursuer, two-evader pursuit evasion differential game," in *49th IEEE conference on decision and control (CDC)*. IEEE, 2010, pp. 3091–3097.
- [16] S.-Y. Liu, Z. Zhou, C. Tomlin, and K. Hedrick, "Evasion as a team against a faster pursuer," in *2013 American control conference*. IEEE, 2013, pp. 5368–5373.
- [17] I. Katz, H. Mukai, H. Schättler, M. Zhang, and M. Xu, "Solution of a differential game formulation of military air operations by the method of characteristics," *Journal of optimization theory and applications*, vol. 125, no. 1, pp. 113–135, 2005.
- [18] K. Shah and M. Schwager, "Multi-agent cooperative pursuit-evasion strategies under uncertainty," in *Distributed Autonomous Robotic Systems*. Springer, 2019, pp. 451–468.
- [19] O. Basimanebottle and X. Xue, "Stochastic optimal control to a nonlinear differential game," *Advances in Difference Equations*, vol. 2014, no. 1, pp. 1–14, 2014.
- [20] M. Pachter and Y. Yavin, "One pursuer and two evaders on the line: A stochastic pursuit-evasion differential game," *Journal of Optimization Theory and Applications*, vol. 39, no. 4, pp. 513–539, 1983.
- [21] Y. Yavin, "A pursuit-evasion differential game with noisy measurements of the evader's bearing from the pursuer," *Journal of optimization theory and applications*, vol. 51, no. 1, pp. 161–177, 1986.
- [22] M. Coon and D. Panagou, "Control strategies for multiplayer target-attacker-defender differential games with double integrator dynamics," in *2017 IEEE 56th Annual Conference on Decision and Control (CDC)*. IEEE, 2017, pp. 1496–1502.
- [23] E. Garcia, D. W. Casbeer, and M. Pachter, "Optimal target capture strategies in the target-attacker-defender differential game," in *2018 Annual American Control Conference (ACC)*. IEEE, 2018, pp. 68–73.
- [24] A. Pierson, Z. Wang, and M. Schwager, "Intercepting rogue robots: An algorithm for capturing multiple evaders with multiple pursuers," *IEEE Robotics and Automation Letters*, vol. 2, no. 2, pp. 530–537, 2016.
- [25] H. Huang, W. Zhang, J. Ding, D. M. Stipanović, and C. J. Tomlin, "Guaranteed decentralized pursuit-evasion in the plane with multiple pursuers," in *2011 50th IEEE Conference on Decision and Control and European Control Conference*. IEEE, 2011, pp. 4835–4840.
- [26] E. Garcia, D. W. Casbeer, A. Von Moll, and M. Pachter, "Cooperative two-pursuer one-evader blocking differential game," in *2019 American Control Conference (ACC)*. IEEE, 2019, pp. 2702–2709.
- [27] V. R. Makkapati and P. Tsiotras, "Optimal evading strategies and task allocation in multi-player pursuit-evasion problems," *Dynamic Games and Applications*, vol. 9, no. 4, pp. 1168–1187, 2019.
- [28] A. Von Moll, M. Pachter, E. Garcia, D. Casbeer, and D. Milutinović, "Robust policies for a multiple-pursuer single-evader differential game," *Dynamic Games and Applications*, vol. 10, no. 1, pp. 202–221, 2020.
- [29] B. Davis, I. Karamouzas, and S. J. Guy, "C-opt: Coverage-aware trajectory optimization under uncertainty," *IEEE Robotics and Automation Letters*, vol. 1, no. 2, pp. 1020–1027, 2016.
- [30] F. Morbidi and G. L. Mariottini, "Active target tracking and cooperative localization for teams of aerial vehicles," *IEEE transactions on control systems technology*, vol. 21, no. 5, pp. 1694–1707, 2012.
- [31] M. Breivik and T. I. Fossen, "Guidance laws for planar motion control," in *2008 47th IEEE Conference on Decision and Control*. IEEE, 2008, pp. 570–577.
- [32] V. R. Makkapati, W. Sun, and P. Tsiotras, "Pursuit-evasion problems involving two pursuers and one evader," in *2018 AIAA Guidance, Navigation, and Control Conference*, 2018, p. 2107.
- [33] A. Ratnoo and T. Shima, "Line-of-sight interceptor guidance for defending an aircraft," *Journal of Guidance, Control, and Dynamics*, vol. 34, no. 2, pp. 522–532, 2011.
- [34] Y. Li, W. Zhang, and X. Liu, "Stability of nonlinear stochastic discrete-time systems," *Journal of Applied Mathematics*, vol. 2013, 2013.
- [35] H. Mania, S. Tu, and B. Recht, "Certainty equivalence is efficient for linear quadratic control," *Advances in Neural Information Processing Systems*, vol. 32, 2019.
- [36] I. M. Tanash and T. Riihonen, "Improved coefficients for the karagiannidis-lioumpas approximations and bounds to the Gaussian Q-Function," *IEEE Communications Letters*, vol. 25, no. 5, pp. 1468–1471, 2021.
- [37] M. López-Benítez and F. Casadevall, "Versatile, accurate, and analytically tractable approximation for the Gaussian Q-function," *IEEE Transactions on Communications*, vol. 59, no. 4, pp. 917–922, 2011.